Desalination and Water Treatment
www.deswater.com
doi: 10.5004/dwt.2023.29312

285 (2023) 289–297
February

Study on the effect of oxidative degradation of Orange G by sonochemical microreactor

Huiyang Liu[a,b], Dong Wang[a,b], Hequn Kang[a,b], Jianfeng Yu[a,b,*]

[a]*Jiangsu Key Laboratory of Advanced Food Manufacturing Equipment and Technology, Wuxi 214122, Jiangsu Province, China, Tel.: +86 13861453545; email: yujf@jiangnan.edu.cn (J. Yu), Tel.: +86 15061885797; email: lhy61885797@126.com (H. Liu), Tel.: +86 18852990396; email: 1239837716@qq.com (D. Wang), Tel.: +86 15581331616; email: 1043200127@stu.jiangnan.edu.cn (H. Kang)*
[b]*School of Mechanical Engineering, Jiangnan University, Wuxi 214122, Jiangsu Province, China*

Received 26 August 2022; Accepted 19 January 2023

ABSTRACT

Azo dye effluent is resistant to conventional wastewater treatment methods, posing severe threats to environmental safety. In the present work, a novel sonochemical microreactor featuring effective ultrasonic transmittance, improved temperature control, and continuous flow processing was designed to achieve efficient degradation of the Orange G (OG). The effects of persulfate dosage, ferrous dosage, initial pH, microchannel width, and ultrasonic power on OG degradation were studied. A maximum degradation efficiency of 96.0% was obtained in sonochemical microreactor degradation system with 6 min of treatment. The 30 s and 6 min degradation efficiency enhanced by ultrasound and microchannel was increased by 9.9% and 2.7%, respectively, compared with the conventional chemistry treatment. The newly designed sonochemical microreactor was clearly proved to have application potential for azo effluent treatment.

Keywords: Azo dye; Degradation efficiency; Sodium persulfate; Sonochemical microreactor; Ultrasound

1. Introduction

Azo dyes are characterised by the presence of at least one azo group (–N=N–), usually linked to aromatic systems and auxochromes [1]. Due to their easy synthesis processes and color fast dyeing effects [2], azo dyes have been widely used in textile [3] and cosmetics industries [4]. However, azo compounds contained in wastewater are usually non-biodegradable, toxic, and potentially carcinogenic [5]. Therefore, the development of efficient technologies for the degradation of azo dyes in the liquid phase is of significant value for environmental protection.

Conventional degradation methods, such as enzyme catalysis [6], biosorption [7], and photocatalysis [8] are time-consuming, uneconomical, and inefficient [9]. In recent years, advanced oxidation processes (AOPs) have been recognized as the most promising wastewater treatment methods [10]. The principle of AOPs is to utilize the strong reactivity of hydroxyl radical ($HO^{\bullet}$) or sulfate radical ($SO_4^{-\bullet}$) to attack organic molecules indiscriminately, thus mineralizing persistent contaminants. Compared with $HO^{\bullet}$, $SO_4^{-\bullet}$ has higher redox potential (2.5–3.1 V vs. 1.8–2.7 V) [11] and longer half-life (30–40 μs vs. 10^{-3} μs) [12]. Azo dyes can be degraded by $SO_4^{-\bullet}$ through C–N bond rupturing [13], desulfurization, and denitrification [14], with carbon dioxide and water as the final products [15]. Therefore, the sulfate radical-based AOPs have been widely considered as reliable wastewater treatment strategies, displaying superior efficiency [16,17].

The use of ferrous ions (Fe^{2+}) activated sodium persulfate (SPS) is one of the common methods to produce $SO_4^{-\bullet}$ in aqueous solution [18]. Because the requisite reagents

* Corresponding author.

are readily available and easy to store [19]. SPS can be activated by Fe^{2+} in accordance with the reactions described by Eqs. (1)–(3) [20,21].

$$2Fe^{2+} + S_2O_8^{2-} \rightarrow 2Fe^{3+} + 2SO_4^{2-} \quad (1)$$

Through the steps:

$$Fe^{2+} + S_2O_8^{2-} \rightarrow Fe^{3+} + SO_4^{-\bullet} + SO_4^{2-} \quad (2)$$

$$SO_4^{-\bullet} + Fe^{2+} \rightarrow Fe^{3+} + SO_4^{2-} \quad (3)$$

Another attractive approach of wastewater treatment is the use of ultrasound, which can result in high mineralization efficiency and short treatment time [22]. The oscillation and cavitation caused by ultrasonic irradiation can promote mixing between solutions and improve the yield of free radicals [23]. According to the hot-spot theory [24], ultrasonic cavitation can produce excessive temperatures and release large amounts of energy, thus promoting a wide range of chemical reactions [25]. The ultrasonic energy input during SPS activation can cause the cleavage of peroxide bonds to produce $SO_4^{-\bullet}$, as displayed in Eq. (4) [12].

$$S_2O_8^{2-} + \text{ultrasonic energy input} \rightarrow 2SO_4^{-\bullet} \quad (4)$$

The ultrasound-assisted AOPs of azo dyes was reported to follow first-order kinetic model, and a degradation efficiency of nearly 95% was achieved within an hour [26]. In addition, the synergistic effect of ultrasound on AOPs was investigated by combining an 860 kHz ultrasound with Fenton treatment to degrade industrial dyes [27]. It was found that the dyes were effectively decomposed into smaller readily degradable molecules due to the enhanced mixing intensity of solutions.

Nevertheless, the aforementioned ultrasonic applications did not form a controllable uniform sound field [28,29] or maximize potential ultrasound utility [30]. As an improved application, sonochemical microreactor combines ultrasound with microchannel, allowing for rapid [31], consecutive [32], efficient [33] and sound-field-controllable degradation [34]. Existing technologies ensure that reactive radicals can be produced in microchannel under the sufficient intensity of ultrasonic irradiation, even without the addition of any other reagents [35]. In order to further optimize the degradation performance of sonochemical microreactor, it is feasible to improve the ultrasonic transmission efficiency and keep the reaction temperature constant.

Thus, the objective of this paper is to design a novel sonochemical microreactor that combines effective ultrasonic transmission and temperature control for the continuous treatment of azo wastewater. $SO_4^{-\bullet}$ was employed as the dominant reactive species. The enhancement effects of cavitation and acoustic streaming phenomena in the microchannels were investigated. The degradation performance of the newly designed sonochemical microreactor was demonstrated. The effects of SPS dosage, Fe^{2+} dosage, initial pH, microchannel width, and ultrasonic intensity on the Orange G (OG) degradation efficiency were evaluated, and optimal parameters were investigated.

2. Materials and methods

2.1. Chemicals and reagents

OG ($C_{16}H_{10}N_2Na_2O_7S_2$) was purchased from the Tianjin Institute of Chemical Reagents (China(. SPS ($Na_2S_2O_8$), ferrous sulfate ($FeSO_4{\cdot}7H_2O$), methanol (CH_3OH), sodium hydroxide (NaOH), and concentrated sulfuric acid (H_2SO_4) were obtained from Sinopharm Chemical Reagent Co., Ltd., (China). All reagents were of analytical grade, and the water used in this study was deionised. The initial concentration of OG was 0.2 mM for all degradation experiments. The solution pH was adjusted by 0.1 M H_2SO_4 and NaOH.

2.2. Experimental instruments

A precision electronic balance (Ningbo Yinzhou Huafeng, China) and a pH meter (Mettler Toledo Instrument, China) were used to configure the experimental reagents. A sonochemical microreactor (Jiangnan University, China), ultrasonic generator (Kemeida Ultrasonic Equipment, China), and dual-channel syringe pump (Suzhou Wenhao Microfluidic Technology, China) were used to form the degradation system. A constant temperature magnetic stirrer (Gongyi Yuhua Instrument, China) and peristaltic pump (Carmel Fluid Technology, China) were used to maintain water circulation to control the reaction temperature. An ultraviolet-visible spectrophotometer (Shimadzu, Japan) was used to measure the absorbance of the degraded solution to calculate the OG degradation efficiency.

2.3. Design of sonochemical microreactor

Fig. 1 shows the diagram of a single sonochemical microreactor, whose enhanced ultrasonic transmission and improved temperature control offered potential applications for wastewater treatment.

2.3.1. Effective ultrasonic transmittance

Ultrasound was delivered at a fixed frequency of 28 kHz, by a customised ultrasonic bath equipped with an ultrasonic oscillator. The maximum ultrasonic power of the oscillator was 100 W. The length, width, and depth of the ultrasonic bath were 200 mm × 125 mm × 6 mm. An acrylic cover plate with a length, width, and thickness of 190 mm × 100 mm × 5 mm was bolted over the bath. Six

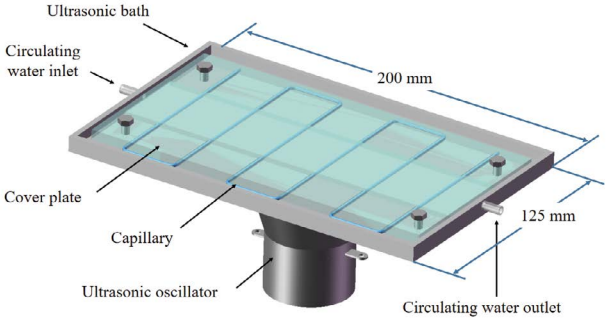

Fig. 1. Diagram of a single sonochemical microreactor.

grooves, spaced 30 mm apart were carved on the bottom surface of the acrylic plate for the capillary inlays. Direct contact between the ultrasonic bath and capillary maximizes the ultrasonic wave transmission.

2.3.2. Improved temperature control

Overheating caused by the continuous operation of the ultrasonic oscillator will negatively affects the degradation performance [36]. To maintain the reaction temperature during sonication, a shallow trough with a depth of 2.5 mm was carved on the bottom surface of the cover plate to provide adequate contact between the circulating water and capillary. Water circulation allowed for the temperature difference between the inlet and outlet of the sonochemical microreactor to remain within 3°C–5°C, which was sufficiently low for the degradation processes in the microchannels not to be affected.

2.4. Design of degradation systems and experimental process

2.4.1. Sonochemical microreactor degradation system

Fig. 2 shows a schematic diagram of a sonochemical microreactor degradation system (SMDS), which was composed of an array of sonochemical microreactors, a peristaltic pump, a dual-channel syringe pump, an ultrasonic generator, capillaries, and receptacles for collecting solutions. The peristaltic pump circulated water from the constant-temperature magnetic stirrer through the ultrasonic bath. The dual-channel syringe pump was used to continuously pump the reagents, with one channel pumping a mixture of ferrous sulfate and OG, and the other channel pumping the SPS solution. A T-joint was used to transfer the reagents into a capillary with an outer diameter of 1.6 mm, and an inner diameter of 0.8, 1.0, or 1.2 mm. To ensure the constant reaction time of solutions in microchannels, the inlet flow rates were 0.8, 1.25 and 1.8 mL/min, for the capillaries with inner diameters of 0.8, 1.0 and 1.2 mm, respectively. In addition, only the last 5 mL of the degraded solution was collected for the measurement. In order to reduce the experimental systematic errors, methanol solution was prepared in advance to quench the residual free radicals in the degraded solution.

2.4.2. Comparative degradation systems

In addition to the SMDS, three other degradation systems including static degradation system (SDS), continuous agitation degradation system (CADS), and microchannel degradation system (MDS) were assembled for comparative studies. The composition of SDS and CADS was the same, with a constant-temperature magnetic stirrer as the major component. In the SDS, solutions of SPS, ferrous sulfate, and OG were poured into a beaker to react at a constant temperature of 25°C. After reaching the specified reaction time, the methanol solution was poured into the beaker for quenching, and the stirring speed was adjusted to 300 rpm to accelerate the termination of the oxidation reaction. The experiments conducted in CADS followed the same procedures as those in SDS, except that the stirring speed was maintained at 300 rpm throughout the experiments. The MDS and SMDS were analogously structured, as visible in Fig. 2. In MDS and SMDS, reagents were continuously injected into the capillary by a dual-channel syringe pump, and a constant reaction temperature was provided through the water circulation. The degraded OG solution flowing out of the capillary was treated as waste liquid, and only the final 5 mL was collected and spectrophotometrically analysed. It should be noted that the ultrasonic oscillators were kept running during the experiments in SMDS, which was prohibited in MDS.

2.5. Evaluation of degradation efficiency

The OG degradation efficiency, η, was used to evaluate the degradation performance of sonochemical microreactor, which was calculated using Eq. (5).

$$\eta = \frac{C_0 - C_t}{C_0} \times 100\% \tag{5}$$

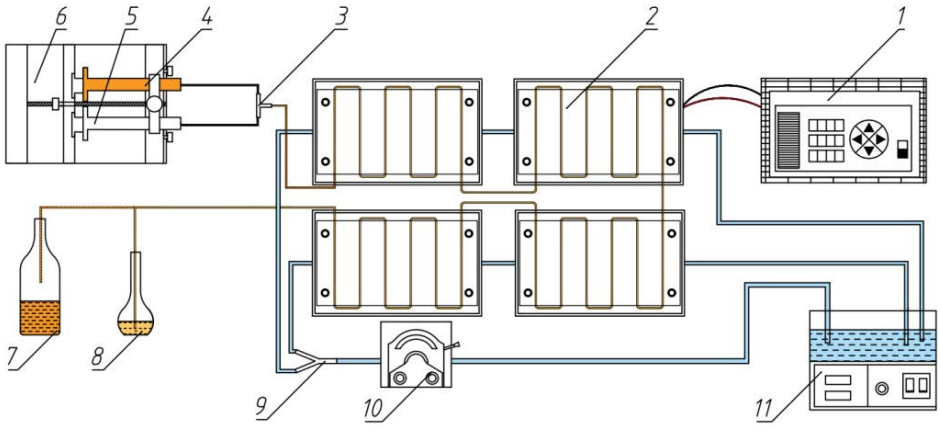

Fig. 2. Schematic representation of the sonochemical microreactor degradation system: 1. ultrasonic generator, 2. sonochemical microreactor array, 3. T-joint, 4. mixed solution of ferrous sulfate and OG, 5. SPS solution, 6. dual-channel syringe pump, 7. collection vial for spent liquor, 8. collection vial for degraded solution, 9. Y-joint, 10. peristaltic pump, and 11. constant-temperature magnetic stirrer.

where C_0 and C_t represent the concentrations of OG before and after the degradation experiment, respectively, in mM.

To determine the OG concentration of degraded solution, 5 mL of experimental sample was taken each time and tested at an absorption wavelength of 478 nm. A calibration plot that relates the absorbance to standard OG concentrations was initially obtained.

2.6. Statistical analysis

Each test sample was measured by taking the average of two measurements to reduce systematic errors during measurement. Origin software was employed for the statistical analysis of the degradation data, and the data points used were the means of replicates. The goodness-of-fit of the absorbance calibration plot was evaluated based on the R^2 value (determination coefficient), where values > 0.99 were considered statistically significant. Analysis of variance (ANOVA) was used to test the significance of the experimental results, and $p < 0.05$ was considered to be statistically significant.

3. Results and discussion

3.1. Effects of different degradation methods on OG degradation

SPS can be thermally activated by ultrasound due to its sonochemical effects, which can promote the formation, growth, and subsequent collapse of cavity bubbles from existing gas nuclei in liquids [37]. In addition, Fe^{2+} can also be used to activate SPS, because the electron transfer by transition metals can promote the generation of PS into $SO_4^{-\bullet}$ [38]. Therefore, the effects of different activation methods of SPS on OG degradation were evaluated.

As depicted in Fig. 3, SPS was activated by ultrasound (US/SPS), Fe^{2+} (Fe^{2+}/SPS), and ultrasound combined with Fe^{2+} (US/Fe^{2+}/SPS). The 5 min degradation efficiency reached 1.3%, 79.9% and 83.2% in US/SPS, Fe^{2+}/SPS and US/Fe^{2+}/SPS systems, respectively. Ultrasound combined with Fe^{2+} brought higher SPS activation efficiency, comparing with the results obtained in US/SPS and US/Fe^{2+}/SPS systems. It can be confirmed that Fe^{2+} was the main species that activated SPS [39]. Additionally, due to the acoustic streaming [23] and ultrasonic cavitation [24] caused by the applied ultrasound, the mixing intensity of the solutions was enhanced, and the $SO_4^{-\bullet}$ yield was improved. Therefore, in US/Fe^{2+}/SPS system, the 5 min degradation efficiency was 3.3% higher than that attained by Fe^{2+}/SPS system.

3.2. Effect of ultrasonic power on OG degradation

Determining an appropriate ultrasonic irradiation intensity contributes to optimizing the operating cost of most physicochemical transformations [40]. In addition, temperature control during sonication is a major requirement for most sonochemical reactions [36]. Despite this, reaction temperature has received little attention from previous studies. Therefore, degradation experiments were conducted in SMDS to investigate the effect of ultrasonic power on OG degradation at varying temperatures.

As evident in Fig. 4, the degradation efficiency at varying reaction temperatures exhibited a similar upward trend. If the vibration amplitude of the ultrasonic oscillators was low, the ultrasonic cavitation cannot be generated, and the mixing of the solution in the capillary was minimally enhanced. So when ultrasonic power was lower than 80 W, the degradation efficiency kept almost constant. When ultrasonic power increased from 80 to 160 W, an obvious increase in OG degradation efficiency was observed, which was attributed to the rapid increase in the intensity of cavitation. However, when ultrasonic power exceeded 160 W,

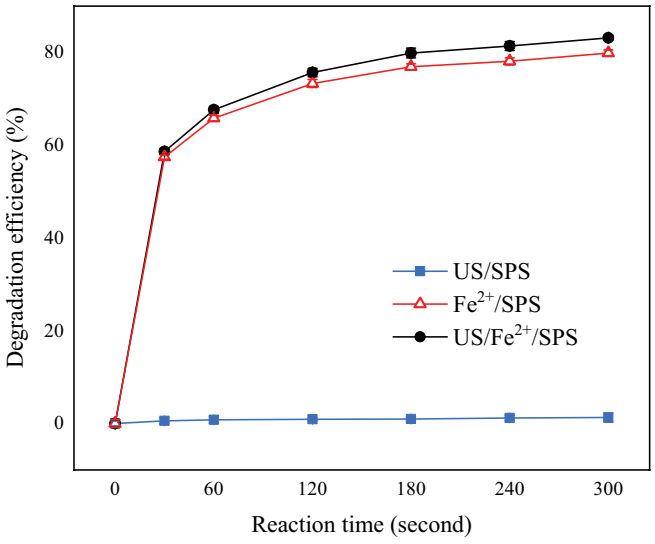

Fig. 3. Effects of different activation methods on OG degradation efficiency (experimental conditions: OG concentration 0.2 mM, Fe^{2+} concentration 0.5 mM, SPS concentration 2.0 mM, initial pH 3, ultrasonic power 400 W, microchannel width 1.0 mm, and reaction temperature 25°C).

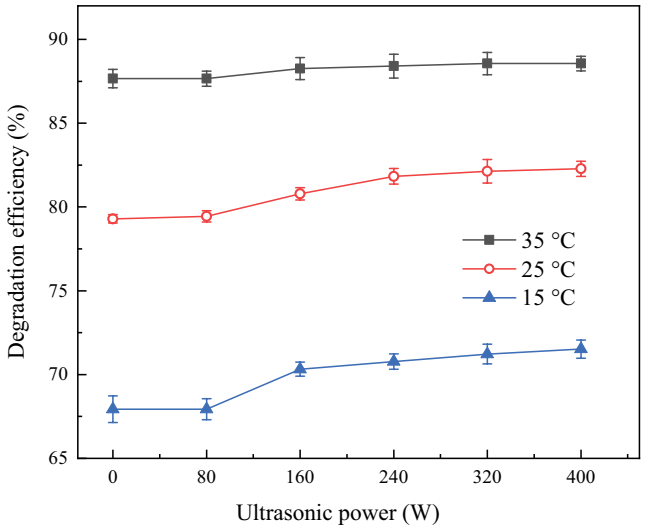

Fig. 4. Effect of ultrasonic power on OG degradation efficiency (experimental conditions: OG concentration 0.2 mM, Fe^{2+} concentration 1.0 mM, SPS concentration 1.0 mM, initial pH 3, ultrasonic power 400 W, microchannel width 1.0 mm, reaction duration 2 min, and reaction temperature 25°C).

the formation of excessive cavitation bubbles reduced the degradation efficiency due to the bubble coalescence, bubble clustering, and acoustic impedance. Therefore, when the ultrasonic power ranged from 160 to 400 W, its influence on OG degradation was not very obvious. Thangavadivel et al. [35] designed a glass microreactor and conducted the ultrasonic assisted degradation experiments of methyl orange (MO). The results showed that when ultrasonic power was lower than 60 W, there was no MO removal. When ultrasonic power increased from 60 to 160 W, the MO degradation efficiency increased from 0 to 9%. When ultrasonic power was increased from 160 to 200 W, the degradation efficiency was increased by less than 0.3%. The conclusion reported by Thangavadivel et al. [35] was highly consistent with that shown in Fig. 4. The degradation efficiency can only be significantly improved by increasing ultrasonic power within a certain range.

3.3. Effect of pH on OG degradation

The process of SPS activated by Fe^{2+} is highly pH-dependent, because Fe^{2+} will precipitate when pH is lower than 4 [41]. However, the application of ultrasound with strong depolymerization is conducive to expanding the pH range of reactions. Therefore, the effect of initial pH on OG degradation was studied in SDS, CADS, MDS, and SMDS.

As visible in Fig. 5, both insufficient and excessive initial pH led to poor degradation performances, and the maximum degradation efficiency was observed at pH of 3. This phenomenon occurred because when the pH was too low, the activation capacity of Fe^{2+} was weakened due to the formation of complex species $[Fe(H_2O)_6]^{2+}$ [42]. Whereas with the increase of solution pH, Fe^{2+} ions precipitated in the aqueous solution, as described by Eq. (6) [43].

$$Fe^{2+} + H_2O \rightarrow Fe(OH)^{+} + H^{+} \quad (6)$$

In the pH range of 1–6, the OG degradation efficiency obtained in SMDS was higher than that of other three degradation systems. In addition, when the initial pH was 4 or 5, the degradation efficiency obtained in MDS and SMDS was higher than that of SDS and CADS. The excellent OG degradation performances achieved in MDS and SMDS were due to the following two reasons. First, the mass transfer intensity between solutions was improved by the micromixing effect caused by microchannel. Second, the utilization of reagents, especially that of Fe^{2+}, was improved because the reagents were pumped continuously into the capillary by a syringe pump. Moreover, the OG degradation efficiency obtained in MDS and SMDS was compared when pH exceeded 4. It was confirmed that both microchannel and ultrasound could delay iron precipitations, thereby improving the OG degradation efficiency.

Admittedly, it is necessary to adjust the solution pH to achieve the highest efficiency of pollutant abatement. However, the required acidic pH is risky from a safety perspective. In order to avoid the potential security risks, some measures need to be considered. For instance, alkaline reagents such as lime solution and sodium hydroxide can be used to neutralize the degraded water. To remove Fe^{2+}/Fe^{3+} precipitates formed during pH adjustment, flocculation [44] and activated carbon adsorption [45] can be used as post-treatment methods.

3.4. Effect of ferrous sulfate dosage on OG degradation

The effect of ferrous sulfate dosage on OG degradation was studied in SDS, CADS, MDS and SMDS. As shown in Fig. 6, the OG degradation efficiency increased gradually when the ferrous sulfate dosage increased from 0.5 to 1.5 mM. The improvement of degradation efficiency was attributed to the rapid generation of $SO_4^{-\bullet}$ caused by the increase in Fe^{2+} concentration [46]. However, the degradation efficiency

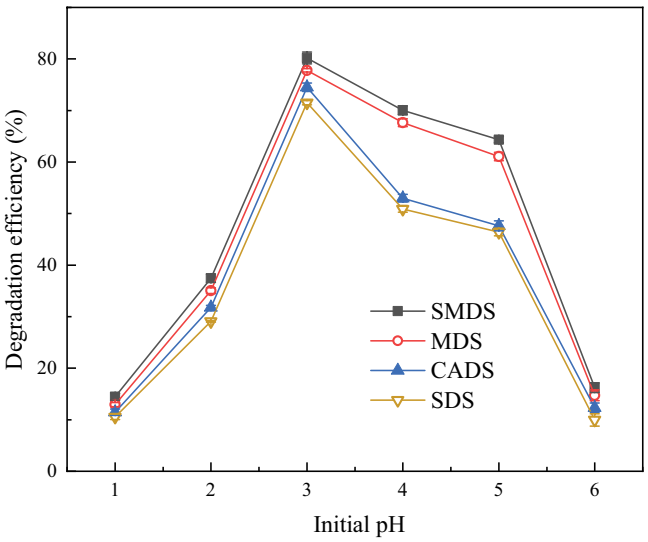

Fig. 5. Effect of initial pH on OG degradation efficiency (experimental conditions: OG concentration 0.2 mM, Fe^{2+} concentration 1.0 mM, SPS concentration 1.0 mM, ultrasonic power 400 W, microchannel width 1.0 mm, reaction duration 2 min, and reaction temperature 25°C).

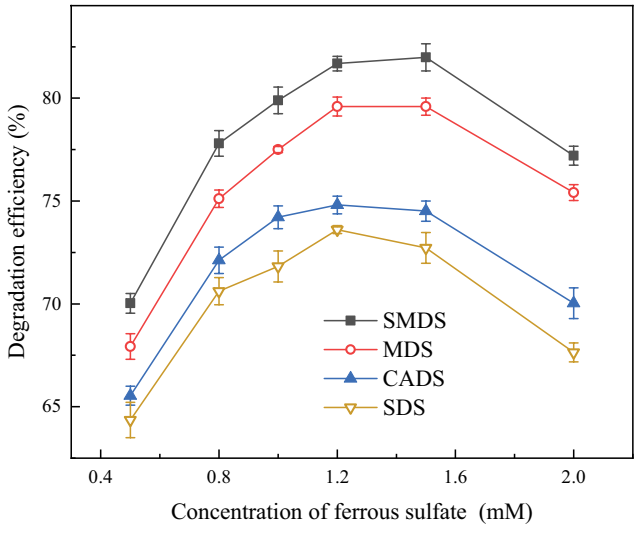

Fig. 6. Effect of ferrous sulfate concentration on OG degradation efficiency (experimental conditions: OG concentration 0.2 mM, SPS concentration 1.0 mM, initial pH 3, ultrasonic power 400 W, microchannel width 1.0 mm, reaction duration 2 min, and reaction temperature 25°C).

decreased as the Fe^{2+} dosage increased from 1.5 to 2.0 mM. A reasonable reason is that surplus Fe^{2+} ions consumed the dominant reactive species $SO_4^{-\bullet}$, as described by Eq. (7) [47].

$$Fe^{2+} + SO_4^{-\bullet} \rightarrow Fe^{3+} + SO_4^{2-} \quad (7)$$

When the ferrous sulfate dosage was 1.5 mM, the degradation efficiency reached 82.0% in SMDS, which was 2.4%, 7.5%, and 9.3% higher than that in MDS, CADS, and SDS, respectively. Different methods of solution mixing led to higher degradation efficiency of SMDS than other systems. SPS, ferrous sulfate, and OG solutions were mixed directly in CADS and SDS. Whereas in SMDS, the reagents were pumped continuously into the capillary for micromixing, increasing the contact area, molecular diffusion, and chaotic convection between species [48]. Since the solutions were uniformly and continuously mixed in SMDS, the effect of excessive local concentration on degradation at the initial stage of the reaction was avoided.

3.5. Effect of sodium persulfate dosage on OG degradation

To investigate the effect of SPS dosage on OG degradation, experiments were conducted in SDS, CADS, MDS and SMDS, with SPS concentrations ranging from 0.5 to 3.0 mM. As depicted in Fig. 7, the trend of degradation efficiency with reaction time was similar in all degradation systems. The OG degradation efficiency increased as SPS concentration increased from 0.5 to 2.0 mM. When SPS dosage was 2.0 mM, 90.1% of degradation efficiency was obtained in SMDS, which was 1.8%, 4.5%, and 6.0% higher than that of MDS, CADS, and SDS, respectively. It can be confirmed that the $SO_4^{-\bullet}$ increased synchronously when SPS dosage increased, thereby bringing a positive effect on OG degradation. However, the iincrease of OG degradation efficiency was less than 2% when the SPS concentration increased from 2.0 to 3.0 mM. As described in Eq. 8, superfluous SPS had little effect on OG degradation owing to the mutual quenching reactions occurring between the excess free radicals. Furthermore, excess PS ions also consumed $SO_4^{-\bullet}$, as described by Eq. (9) [49].

$$SO_4^{-\bullet} + SO_4^{-\bullet} \rightarrow 2SO_4^{2-} \quad (8)$$

$$S_2O_8^{2-} + SO_4^{-\bullet} \rightarrow SO_4^{2-} + S_2O_8^{-} \quad (9)$$

3.6. Effect of microchannel width on OG degradation

For a sonochemical microreactor, the microchannel width is one of the important factors that affects the inlet flow rate, solution dosage, and mixing intensity in the microchannel [48]. Hence, the effect of microchannel width on OG degradation was studied in SMDS, and the results are presented in Fig. 8. The degraded solutions were collected at time intervals of 30 s for up to 3 min and stored in vials pre-filled with methanol to quench residual oxidants.

As illustrated in Fig. 8, under silent treatment, the degradation efficiency reached 65.7%, 70.6% and 73.9% when the microchannel widths were 0.8, 1.0 and 1.2 mm, respectively. When 400 W ultrasonic power was applied, the corresponding degradation efficiency was increased to 67.6%, 73.2% and 76%, respectively. As the microchannel width increased from 0.8 to 1.2 mm, the Reynolds (Re) number of microfluidic in microchannel increased from 21.2 to 31.9. Since higher Re number means more intense solution mixing [48], the OG degradation efficiency therefore increased with the increase of microchannel width. Additionally, the enhancement effect of ultrasound on OG degradation was more obvious in wider microchannel. The increase

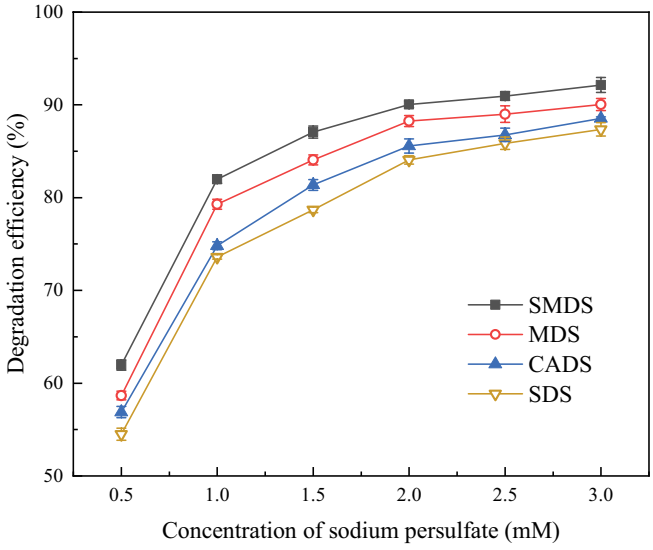

Fig. 7. Effect of sodium persulfate concentration on OG degradation efficiency (experimental conditions: OG concentration 0.2 mM, Fe^{2+} concentration 1.2 mM, ultrasonic power 400 W, initial pH 3, microchannel width 1.0 mm, reaction duration 2 min, and reaction temperature 25°C).

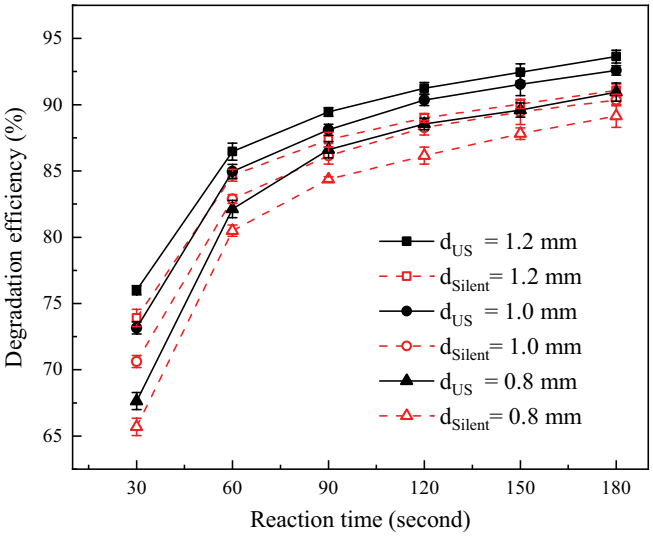

Fig. 8. Effect of microchannel width on OG degradation efficiency with and without ultrasound (experimental conditions: OG concentration 0.2 mM, Fe^{2+} concentration 1.2 mM, SPS concentration 2.0 mM, initial pH 3, ultrasonic power 400 W, and reaction temperature 25°C).

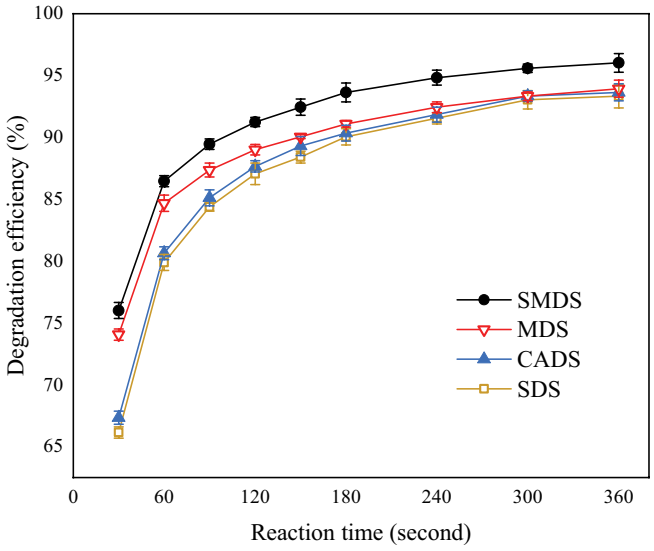

Fig. 9. OG degradation efficiency in SMDS, MDS, CADS and SDS (experimental conditions: OG concentration 0.2 mM, Fe^{2+} concentration 1.2 mM, SPS concentration 2.0 mM, initial pH 3, ultrasonic power 400 W, microchannel width 1.2 mm, and reaction temperature 25°C).

of acoustic cavitation intensity caused by the increase of ultrasonic power was more obvious in wide channel than in narrow channel. The phenomenon of the decreased channel dimension restrained the acoustic cavitation intensity was also be demonstrated in literature [34].

3.7. Degradation efficiency of OG in different degradation systems

In order to evaluate the enhancement effect of sonochemical microreactor on OG degradation, comparative experiments were performed in SDS, CADS, MDS, and SMDS. As evident in Fig. 9, the SMDS equipped with the newly designed sonochemical microreactor maintained a higher degradation efficiency than the other three systems within 6 min. In SMDS, the 6 min degradation efficiency was 96.0%, which was 2.7%, 2.4%, and 2.1% higher than that in SDS, CADS, and MDS, respectively. Additionally, at the initial stage of degradation, a significant enhancement effect of sonochemical microreactor was also observed. Specifically, 76.0% of OG were degraded within 30 s in SMDS, while the corresponding degradation efficiency was only 66.1%, 67.3% and 74.1% in SDS, CADS, and MDS, respectively. By comparing the results obtained in SMDS and SDS, it was confirmed that the 30 sec and 6 min degradation efficiency was increased by 9.9% and 2.7% due to the application of sonochemical microreactor.

An obvious removal of OG was observed at the beginning of the degradation, as more than 80% of the OG was degraded within 1 min. Since OG and $SO_4^{\bullet-}$ in aqueous solution were rapidly reduced, the microchannel and ultrasound did not remarkably promote the OG degradation. Anyhow, the highest degradation efficiency observed in SMDS confirmed the application prospect of sonochemical microreactor in wastewater treatment.

4. Conclusions

The OG degradation performance of a novel sonochemical microreactor was investigated by optimizing the reagent dosage, initial pH, microchannel width, and ultrasonic intensity to maximize degradation efficiency. The results were showed that the degradation efficiency increased with an increasing ultrasonic power, SPS dosage and microchannel width. As the Fe^{2+} dosage and initial pH increased, the degradation efficiency initially increased and then decreased. A maximum degradation efficiency of 96.0% was obtained in SMDS, at reaction time of 6 min, OG concentration of 0.2 mM, Fe^{2+} concentration of 1.2 mM, SPS concentration of 2.0 mM, initial pH of 3, ultrasonic power of 400 W, microchannel width of 1.2 mm, and reaction temperature of 25°C. By comparing the degradation efficiency obtained in SMDS and SDS, it can be confirmed that 30 s and 6 min degradation efficiency was improved by 9.9% and 2.7%, respectively, due to the combination of ultrasound and microchannel. The newly designed sonochemical microreactor was proved to meet the requirements for the efficient degradation of azo pollutants. Further research on sonochemical microreactors with large throughput and multiple channels will be useful to the future development of wastewater treatment technology.

Conflict of interest

The authors declare that they have no conflict of interest.

Data availability

The data that support the findings of this study are available from the corresponding author, upon reasonable request.

Acknowledgments

The authors would like to thank Wuxi Hesen Technology Co., Ltd for providing ultrasonic oscillators and technical supports.

Funding

No funding was received to assist with the preparation of this manuscript.

References

[1] M. Cai, J. Su, G. Lian, G. Lian, X. Wei, C. Dong, H. Zhang, M. Jin, Z. Wei, Sono-advanced Fenton decolorization of azo dye Orange G: analysis of synergistic effect and mechanisms, Ultrason. Sonochem., 31 (2016) 193–200.
[2] R.I. Alsantali, Q.A. Raja, A.Y.A. Alzahrani, A. Sadiq, N. Naeem, E.U. Mughal, M.M. Al-Rooqi, N.E. Guesmi, Z. Moussa, S.A. Ahmed, Miscellaneous azo dyes: a comprehensive review on recent advancements in biological and industrial applications, Dyes Pigm., 199 (2022) 110050, doi: 10.1016/j.dyepig.2021.110050.
[3] S. Benkhaya, S. M'Rabet, A.E. Harfi, Classifications, properties, recent synthesis and applications of azo dyes, Heliyon, 6 (2020) e03271, doi: 10.1016/j.heliyon.2020.e03271.
[4] L. Xu, X. Zhou, G. Wang, L. Zhou, X. Sun, Catalytic degradation of acid red B in the system of ultrasound/peroxymonosulfate/

Fe_3O_4, Sep. Purif. Technol., 276 (2021) 119417, doi: 10.1016/j.seppur.2021.119417.
[5] S. Kodavatiganti, A.P. Bhat, P.R. Gogate, Intensified degradation of Acid violet 7 dye using ultrasound combined with hydrogen peroxide, Fenton, and persulfate, Sep. Purif. Technol., 279 (2021) 119673, doi: 10.1016/j.seppur.2021.119673.
[6] S. Bakhshian, H. Kariminia, R. Roshandel, Bioelectricity generation enhancement in a dual chamber microbial fuel cell under cathodic enzyme catalyzed dye decolorization, Bioresour. Technol., 102 (2011) 6761–6765.
[7] E.B. Guari, R. Janaina, M.S. Martiarena, N.S. Yamagami, C.R. Corso, Azo dye acid blue 29: biosorption and phytotoxicity test, Water Air Soil Pollut., 226 (2015) 361, doi: 10.1007/s11270-015-2611-3.
[8] P. Ezhilkumar, V.M. Sivakumar, M. Thirumarimurugan, Degradation of formaldehyde from wastewater by batch re-circulation process using a photocatalytic reactor, Desal. Water Treat., 243 (2021) 206–210.
[9] M.P. Rayaroth, C.T. Aravindakumar, N.S. Shah, G. Boczkaj, Advanced oxidation processes (AOPs) based wastewater treatment - unexpected nitration side reactions - a serious environmental issue: a review, Chem. Eng. J., 430 (2021) 133002, doi: 10.1016/j.cej.2021.133002.
[10] H. Kusic, I. Peternel, S. Ukic, N. Koprivanac, T. Bolanca, S. Papic, A.L. Bozic, Modeling of iron activated persulfate oxidation treating reactive azo dye in water matrix, Chem. Eng. J., 172 (2011) 109–121.
[11] T. Olmez-Hanci, I. Arslan-Alaton, Comparison of sulfate and hydroxyl radical based advanced oxidation of phenol, Chem. Eng. J., 224 (2013) 10–16.
[12] N. Liu, F. Ding, C.C. Weng, Y.T. Lin, Effective degradation of primary color direct azo dyes using Fe^0 aggregates-activated persulfate process, J. Environ. Manage., 206 (2018) 565–576.
[13] K. Shamsabadi, M. Behpour, Comparing photocatalytic activity consisting of Sb_2S_3 and Ag_2S on the TiO_2-SiO_2/TiO_2 nanotube arrays-support for improved visible-light-induced photocatalytic degradation of a binary mixture of basic blue 41 and basic red 46 dyes, Int. J. Hydrogen Energy, 46 (2021) 26989–27013.
[14] O.O. Wahab, L.O. Olasunkanmi, K.K. Govender, P.P. Govender, A DFT study of disperse Yellow 119 degradation mechanism by hydroxyl radical attack, ChemistrySelect, 3 (2018) 12988–12997.
[15] G.A. Ismail, H. Sakai, Review on effect of different type of dyes on advanced oxidation processes (AOPs) for textile color removal, Chemosphere, 291 (2022) 132906, doi: 10.1016/j.chemosphere.2021.132906.
[16] X. Lin, Y. Ma, J. Wan, Y. Li, Efficient degradation of Orange G with persulfate activated by recyclable $FeMoO_4$, Chemosphere, 214 (2018) 642–650.
[17] M.Y. Kilic, W. Abdelraheem, X. He, K. Kestioglu, D.D. Dionysiou, Photochemical treatment of tyrosol, a model phenolic compound present in olive mill wastewater, by hydroxyl and sulfate radical-based advanced oxidation processes (AOPs), J. Hazard. Mater., 367 (2019) 734–742.
[18] S. Kaya, Y. Asci, Application of heterogeneous Fenton processes using Fe(III)/MnO_2 and Fe(III)/SnO_2 catalysts in the treatment of sunflower oil industrial wastewater, Desal. Water Treat., 171 (2019) 302–313.
[19] Z. Yan, Y. Gu, X. Wang, Y. Hu, X. Li, Degradation of aniline by ferrous ions activated persulfate: impacts, mechanisms, and by-products, Chemosphere, 268 (2020) 129237, doi: 10.1016/j.chemosphere.2020.129237.
[20] C.G. Niu, Y. Wang, X.G. Zhang, G.M. Zeng, D.W. Huang, R. Min, X.W. Li, Decolorization of an azo dye Orange G in microbial fuel cells using Fe(II)-EDTA catalyzed persulfate, Bioresour. Technol., 126 (2012) 101–106.
[21] S. Wang, J. Wu, X. Lu, W. Xu, Q. Gong, J. Ding, B. Dan, P. Xie, Removal of acetaminophen in the Fe^{2+}/persulfate system: kinetic model and degradation pathways, Chem. Eng. J., 358 (2018) 1091–1100.
[22] A. Abdelhay, M.A. Allawzi, B. Al-Khateeb, A. Albsoul, A.A. Othman, Optimization of the performance of ultrasonic irradiation for the treatment of textile wastewater: synergetic effect of US and advanced oxidation, Water Air Soil Pollut., 233 (2022) 1–18.
[23] M. Moradi, A. Elahinia, Y. Vasseghian, E.N. Dragoi, A.M. Khaneghah, A review on pollutants removal by sonophoto-Fenton processes, J. Environ. Chem. Eng., 8 (2020) 104330, doi: 10.1016/j.jece.2020.104330.
[24] S. Giray, M.H. Morcali, S. Akarsu, C.A. Ziba, M. Dolaz, Comparison of classic Fenton with ultrasound Fenton processes on industrial textile wastewater, Sustain. Environ. Res., 28 (2018) 165–170.
[25] A. Hassani, M. Malhotra, A.V. Karim, S. Krishnan, P.V. Nidheesh, Recent progress on ultrasound-assisted electrochemical processes: a review on mechanism, reactor strategies, and applications for wastewater treatment, Environ. Res., 205 (2021) 112463, doi: 10.1016/j.envres.2021.112463.
[26] P. Gayathri, R.P.J. Dorathi, K. Palanivelu, Sonochemical degradation of textile dyes in aqueous solution using sulphate radicals activated by immobilized cobalt ions, Ultrason. Sonochem., 17 (2010) 566–571.
[27] A. Maroudas, P.K. Pandis, A. Chatzopoulou, L.R. Davellas, C. Argirusis, Synergetic decolorization of azo dyes using ultrasounds, photocatalysis and photo-Fenton reaction, Ultrason. Sonochem., 71 (2021) 105367, doi: 10.1016/j.ultsonch.2020.105367.
[28] Z.Y. Dong, C. Delacour, K.M. Carogher, A.P. Udepurkar, S. Kuhn, Continuous ultrasonic reactors: design, mechanism and application, Materials, 13 (2020) 344, doi: 10.3390/ma13020344.
[29] P.R. Gogate, Cavitational reactors for process intensification of chemical processing applications: a critical review, Chem. Eng. Process, 47 (2008) 515–527.
[30] J.J. John, S. Kuhn, L. Braeken, T.V. Gerven, Ultrasound assisted liquid-liquid extraction in microchannels - a direct contact method, Chem. Eng. Process. Process Intensif., 102 (2016) 37–46.
[31] K.M. Carogher, Z. Dong, D.S. Stephens, M.E. Leblebici, S. Kuhn, Acoustic resonance and atomization for gas-liquid systems in microreactors, Ultrason. Sonochem., 75 (2021) 105611, doi: 10.1016/j.ultsonch.2021.105611.
[32] G. Dong, B. Chen, B. Liu, L.J. Hounjet, Y. Cao, S.R. Stoyanov, M. Yang, B. Zhang, Advanced oxidation processes in microreactors for water and wastewater treatment development, challenges, and opportunities, Water Res., 211 (2022) 118047, doi: 10.1016/j.watres.2022.118047.
[33] K. Fedorov, K. Dinesh, X. Sun, R.D.C. Soltani, Z. Wang, S. Sonawane, G. Boczkaj, Synergistic effects of hybrid advanced oxidation processes (AOPs) based on hydrodynamic cavitation phenomenon - a review, Chem. Eng. J., 432 (2022) 134191, doi: 10.1016/j.cej.2021.134191.
[34] S. Zhao, C. Yao, Z. Dong, G. Chen, Q. Yuan, Role of ultrasonic oscillation in chemical processes in microreactors: a mesoscale issue, Particuology, 48 (2020) 88–99.
[35] K. Thangavadivel, M. Konagaya, K. Okitsu, M. Ashokkumar, Ultrasound-assisted degradation of methyl orange in a micro reactor, J. Environ. Chem. Eng., 2 (2014) 1841–1845.
[36] J.J. John, S. Kuhn, L. Braeken, T.V. Gerven, Temperature controlled interval contact design for ultrasound assisted liquid-liquid extraction, Chem. Eng. Res. Des., 125 (2017) 146–155.
[37] L.W. Matzek, K.E. Carter, Activated persulfate for organic chemical degradation: a review, Chemosphere, 151 (2016) 178–188.
[38] J. Wang, S. Wang, Activation of persulfate (PS) and peroxymonosulfate (PMS) and application for the degradation of emerging contaminants, Chem. Eng. J., 334 (2018) 1502–1517.
[39] D. Han, J. Wan, Y. Ma, Y. Wang, M. Huang, Y. Chen, D. Li, Z. Guan, Y. Li, Enhanced decolorization of Orange G in a Fe(II)-EDDS activated persulfate process by accelerating the regeneration of ferrous iron with hydroxylamine, Chem. Eng. J., 256 (2014) 316–323.
[40] P.R. Gogate, V.S. Sutkar, A.B. Pandit, Sonochemical reactors: important design and scale up considerations with a special emphasis on heterogeneous systems, Chem. Eng. J., 166 (2011) 1066–1082.
[41] J. Theerthagiri, J. Madhavan, S.J. Lee, M.Y. Choi, B.G. Pollet, Sonoelectrochemistry for energy and environmental

applications, Ultrason. Sonochem., 63 (2020) 104960, doi: 10.1016/j.ultsonch.2020.104960.
[42] X.R. Xu, Z.Y. Zhao, X.Y. Li, J.D. Gu, Chemical oxidative degradation of methyl tert-butyl ether in aqueous solution by Fenton's reagent, Chemosphere, 55 (2004) 73–79.
[43] X.R. Xu, X.Z. Li, Degradation of azo dye Orange G in aqueous solutions by persulfate with ferrous ion, Sep. Purif. Technol., 72 (2010) 105–111.
[44] X. Xiao, Y. Sun, W. Sun, H. Shen, H. Zheng, Y. Xu, J. Zhao, H. Wu, C. Liu, Advanced treatment of actual textile dye wastewater by Fenton-flocculation process, Can. J. Chem. Eng., 95 (2017) 1245–1252.
[45] M. Sgroi, F. Vagliasindi, S.A. Snyder, P. Roccaro, N-Nitrosodimethylamine (NDMA) and its precursors in water and wastewater: a review on formation and removal, Chemosphere, 241 (2018) 685–703.
[46] L. Bu, Z. Shi, S. Zhou, Modeling of Fe(II)-activated persulfate oxidation using atrazine as a target contaminant, Sep. Purif. Technol., 169 (2016) 59–65.
[47] D. Han, J. Wan, Y. Ma, Y. Wang, Y. Li, D. Li, Z. Guan, New insights into the role of organic chelating agents in Fe(II) activated persulfate processes, Chem. Eng. J., 269 (2015) 425–433.
[48] J. Liang, J.F. Yu, Y. Cheng, Y. Wu, Y. Li, Electrochemical detection of baicalein based on a three-dimensional micromixer, J. Micromech. Microeng., 30 (2020) 125017, doi: 10.1088/1361-6439/abc52d.
[49] W. Shang, Z. Dong, M. Li, X. Song, M. Zhang, C. Jiang, F. Sun, Degradation of diatrizoate in water by Fe(II)-activated persulfate oxidation, Chem. Eng. J., 361 (2019) 1333–1344.